Constant Pressure Specific Heat to Hemispherical Total Emissivity Ratio for Undercooled Liquid Nickel, Zirconium, and Silicon

Aaron J. Rulison* and Won-Kyu Rhim

Jet F'repulsion Laboratory
M/C 183-401
4800 Oak Grove Drive
Pasadena, CA 91109

● National Research Council Resident Research Associate

For publication in *Metallurgical and Materials Transactions B: Process Metallurgy and Materials Processing Science.*

Abstract

Radiative cooling curves of nickel, zirconium, and silicon melts which were obtained using the High Temperature High Vacuum Electrostatic Levitator have been analyzed to determine the ratio between the constant pressure specific heat and the hemispherical total emissivity, $c_p(T)/\varepsilon_T(T)$. This ratio determined over a wide liquid temperature range for each material allows us to determine $c_p(T)$ if $\varepsilon_T(T)$ is known, or vice versa. Following the recipe, the hemispherical total emissivities for each sample at its melting temperature, $\varepsilon_T(T_m)$, have been determined using $c_p(T_m)$ values available in the literature. They are 0.15, 0.29, and 0.17, for Ni, Zr, and Si, respectively.

Introduction

Data on both constant pressure specific heat c_p and hemispherical total emissivity ε_T of undercooled liquids are important parameters for studies of phase transformation into various solid phases which exhibit a range of physical and chemical properties.

The constant pressure specific heat is defined as the first derivative of specific enthalpy, h, with respect to temperature at constant pressure, i.e.,

$$c_p = \left(\frac{\partial h}{\partial T}\right)_p \quad . \tag{1}$$

The temperature dependence of c_p is needed to calculate the thermodynamic state functions such as enthalpy, entropy, Gibbs free energy, etc. For example, c_p through its influence on the Gibb's free energy determines the depth of undercooking reached before the onset of solid phase nucleation. The depth of undercooking allows us to control the phases and microstructure of the solid product [1].

The total hemispherical emissivity of a sample, ε_T, is defined as the ratio of its hemispherical total emissive power, H, to that of a black body, i.e.,

$$\varepsilon_T = \frac{H}{\sigma T^4}, \tag{2}$$

where σ is the Stefan-Boltzmann constant (5.670×10^{-8} W m^{-2} K^{-4}) and T is the absolute temperature [2]. Data on ε_T are needed to calculate radiant heat fluxes. For example, ε_T determines the thermal environment during crystal growth in the floating zone growth system. It also plays an important role in determining the cooling rate of atomized droplets in rapid solidification processing. In addition, ε_T data may serve as a bridge to other materials properties. The relationship between ε_T and the electrical resistivity, r_e, in metals has been explored by a number of researchers [3]. Data on

both ε_T and r_e at a given temperature should, in principle, allow calculation of the electronic transport properties of the metals, i.e., the effective number of free electrons per unit volume, N_{eff}, and the electronic relaxation time, τ. These two quantities determine much of the behavior and properties of a metal.

In spite of their importance, c_p and ε_T are known for very few high-temperature liquids. This is due to the difficulties of maintaining pure liquids at high temperatures. Data is particularly scarce for undercooked liquids since they immediately solidify when placed in contact with most crucibles. These problems are avoided, however, using the recently-developed high-temperature, high-vacuum electrostatic levitator (HTHVESL) described below [4]. The HTHVESL allows accurate determination of c_p/ε_T in a simple heat transfer environment while the levitated melt cools to a deeply undercooked state. In the HTHVESL, levitated materials can be melted, undercooked, and solidified in vacuum. Under such conditions deeply undercooked liquids can be maintained for significant periods of time.

The present letter describes the methodology for measuring $c_p(T)/\varepsilon_T(T)$ using the HTHVESL. Results are presented for two pure metals and one semiconductor in their liquid states over the temperature range which includes undercooked regions. The data can readily be used to determine either parameter if the other is available. Following a brief description of the experimental approach the temperature dependence of $c_p(T)/\varepsilon_T(T)$ and $\varepsilon_T(T_m)$ are given for liquid nickel, zirconium, and silicon.

Measurement Approach

The HTHVESL levitates 1 to 3 mm diameter samples between parallel plate electrodes in a stainless steel chamber which is typically evacuated to 10-8 to 10^{-6} Torr Positioning of a charged sample is achieved through the application of feedback-controlled electrostatic fields that are generated by a set of electrodes

around the sample (Fig. 1). The vertical electric field, used for generating the force which counteracts gravity, is provided by the top and bottom electrodes which are circular, 25 mm in diameter, and positioned co-axially, 10 mm apart. The surface of the top electrode is flat. The surface of the bottom electrode is very slightly conical, sloping down toward the center at 2° with respect to horizontal, so that a round sample will roll to the center when it is not being levitated. Four 6 mm diameter, 9 mm long cylindrical side electrodes with rounded ends are spaced 90° apart around the bottom electrode to provide positioning control in the horizontal plane.

The electrode assembly lies approximately at the center of the surrounding stainless steel vacuum chamber. The inside surface of the vacuum chamber forms a 25 cm diameter, 20 cm high cylinder with a vertical axis. Samples are heated using a 1-kW xenon arc lamp whose radiation is focussed through a 5 cm diameter quartz lens placed 7.5 cm from the sample. A 7.5 cm diameter concave mirror with a 7.5 cm radius of curvature is placed 7.5 cm from the sample opposite the lens. The mirror increases heating efficiency by refocusing radiation which came through the lens but missed the sample on the first pass. Of course, the mirror also focuses radiation emitted by the sample during radiative cooling back onto the sample, thereby affecting the radiative cooling rate. The mirror's affect on the measured $c_p(T)/\varepsilon_T(T)$ from this effect will be discussed below.

Once molten, the samples maintain a very nearly spherical shape due to the action of surface tension. Since the molten samples are levitated in vacuum, all sources of impurities are eliminated and a clean surface can be maintained.

In order to maintain clean surfaces during processing, it was necessary to begin with pure, clean samples. Clean samples were prepared from high purity stock materials using specific cleaning treatments after cutting and grinding the material to the appropriate size.

Nickel: A piece of shot from ESPI, Inc., of 99.99% nominal purity, was roughly ground to sphere. It was washed for 1 minute in a solution at room temperature consisting of 1 part by volume distilled water, 1.5 parts by volume sulfuric acid, 2.25 parts by volume nitric acid, and 6 g/1 sodium chloride. It was then rinsed in distilled water, 2% ammonia, and finally anhydrous ethanol. The sample's mass was 19.4 mg.

Zirconium: A chunk of nominally 99.95°A pure stock was obtained from Teledyne Wah-Chang, Albany, Oregon, and prepared by arc-melting in an argon atmosphere on a water-cooled plate to form it into an approximate sphere. It was then cleaned for 15 seconds in a solution at room temperature consisting of 40% nitric acid, 5% hydrofluoric acid, and 55% water (by volume). This was followed by a rinse in distilled water, and a final rinse in anhydrous ethanol. The sample's mass was 40.7 mg.

Silicon: Samples were cut from nominally 99.9995°/0 pure stock from Johnson-Matthey. These were then ground roughly into spheres. They were cleaned by immersion in 50% HF at room temperature for 5 minutes, rinsed in distilled water, and finally rinsed in anhydrous ethanol. The samples' masses were 8.9, 17.2, 23.3, 31.9, and 45.2 mg.

Samples prepared in the above manner showed no impurity particles or patches on their surfaces even under brilliant illumination from the xenon arc lamp.

Figure 2 shows the temperature vs. time (as measured by the pyrometer described below) during cooling of a levitated nickel sphere of 19.4 mg. To begin, the levitated sample was melted and heated about 100 K above its melting temperature using the arc lamp. Then the lamp was completely blocked (see point #1, Fig. 2) and the sample began to cool. The sample was levitated in the vacuum chamber with gas pressure less than 10^{-6} Torr. Evaporative cooling was negligible. Therefore, the heat transfer was almost purely radiative. In Fig. 2, the sample reached its melting temperature at point #2 and undercooked to point #3 where solid phase nucleation occurred. The latent heat of fusion was released between points #3 and #4, raising

the sample's temperature to T_m. The sample was completely solid by point #5 after which it cooled to point #6 at which the measurement was terminated.

The temperature of each sample was determined using a single-color pyrometer operated in the manner described by Hofmeister et al. [5]. The pyrometer gathers thermal radiation emitted from -1 mm^2 circular region on the sample. The radiation is directed through a 658 nm optical filter with 10 nm FWHM. The filtered light falls onto a silicon photodiode which, with associated electronics, provides a voltage, V_{out}, which is linearly proportional to the intensity. According to Planck's equation for the spectral radiance of a thermally-radiating body,

$$V_{out} = \frac{2\pi C_1 \varepsilon_\lambda K}{\lambda^5 [exp(C_2/\lambda T) - 1]} \tag{3}$$

where Cl is O.59544Xl 0^{-16} $W \cdot m^2$, ε_λ is the normal spectral emissivity of the sample (which in general may be a function of temperature), K is an instrument constant, C_2 is 1.4388x104 $\mu m \cdot K$, λ is the wavelength, and T is the absolute temperature [2]. If V_{out} is measured at a reference point in time, t_{ref}, when the sample temperature is known, then Eq. (3) leads to the following expression for the temperature at any other time, assuming $exp(C_2/\lambda T) >> 1$:

$$T(t) = \frac{1}{\frac{1}{T(t_{ref})} + \frac{\lambda}{C_2} ln\left[r_\lambda(t) \frac{V_{out}(t_{ref}) - V_b}{V_{out} - V_b}\right]} \tag{4}$$

where $r_\lambda(t) = \varepsilon_\lambda(t)/\varepsilon_\lambda(t_{ref})$, and V_b is the zero-light pyrometer signal. Note that ε_λ need not be known at any time, but its relative change over time must be known in order to specify r_λ.

To proceed, we assumed that, as long as the sample remained liquid, ε_λ was not a function of time (i.e. $r_\lambda = 1$) . (The error introduced into the measurements from this assumption will be discussed below.) Furthermore, for Ni and Zr we found that V_{out} was very nearly constant in the post-recalescence isotherm during which the sample converts from a liquid/solid mix to completely solid. Since the sample maintains T_m during the post-recalescence isotherm, this indicates that the normal spectral emissivity of liquid and solid at T_m were the same. In that case, Eq. (4) for liquid Ni and Zr becomes the following expression which applies over the entire cooling curve:

$$T = \frac{1}{\frac{1}{T_m} + \frac{\lambda}{C_2} \ln\left[(V_{out}(T_m) - V_b)/(V_{out} - V_b)\right]} \qquad (5)$$

where T_m was chosen as the reference temperature.

Unlike Ni and Zr, Si showed a marked increase in radiance during the post-recalescence isotherm as the sample converted from a mixture of liquid and solid to completely solid. This indicates that the normal spectral emissivity of the solid at T_m is greater than that of the liquid at T_m. To account for the varying emissivity, we chose solid silicon at T_m as the reference pyrometer output. Thus Eq. (4) for liquid Si becomes

$$T(t) = \frac{1}{\frac{1}{T_m} + \frac{\lambda}{C_2} \ln \frac{\varepsilon_{\lambda\cdot liquid}}{\text{'A-solid}} \frac{V_{out}(T_{m,solid}) - V_b}{V_{out} - V_b}} \qquad (6)$$

where $\varepsilon_{\lambda\cdot liquid}$ and $\varepsilon_{\lambda\cdot solid}$ are the normal spectral emissivities at T_m and 658 nm in the liquid and solid states, respectively. Data on $\varepsilon_{\lambda\cdot liquid}$ and $\varepsilon_{\lambda\cdot solid}$ are not available at 658 nm, but data at 632.8 nm are available and were used as a first approximation. Using data from Krishnan et al. [6], we estimate $\varepsilon_{\lambda\cdot liquid}/\varepsilon_{\lambda\cdot solid}$ = ().42.

As stated above, the spectral emissivity for Ni, Zr, and Si was assumed to be temperature-independent in the liquid state. The error introduced into the temperature measurement from this assumption was investigated by Krishnan et al. [6]. Using their results for liquid Si, it is estimated that the constant spectral emissivity introduces less than 4 K error at the present undercooling limit. This translates to an error of less than 3% in the computed c_p/ε_T. The error introduced into the Ni and Zr results by the constant spectral emissivity assumption is unknown at this time but is probably less than a few percent.

Now we turn our attention to the measurement of c_p/ε_T. The approach has been called the "transient calorimetric technique" [7], Because each sample is processed in vacuum and because electrostatic levitation does not affect the internal energy of the sample, a particularly simple expression for conservation of energy can be written:

$$\frac{mc_p}{M}\frac{dT}{dt} = -\varepsilon_T \sigma A(T^4 - T_c^4) \qquad (7)$$

where m is the sample's mass, M is its molecular weight, A is its total surface area, and T_c is the vacuum chamber temperature which was approximately 50°C. Equation (7) involves several assumptions. First, it is assumed that the hemispherical total absorptivity of the sample absorbing radiation from a black body at T_c is equal to the sample's hemispherical total emissivity at T, i.e., the sample is a gray body. This approximation introduces little error since $T^4 >> T_c^4$. That is, the sample need not be a gray body for the present method to give accurate results. (Note that the top electrode was indirectly heated by the xenon to about 100°C, while the surrounding chamber was at about 50°C. Given the much higher sample temperatures, the higher temperature of the top electrode had negligible affect on heat transfer to the sample.) Another effect is neglected in deriving Eq. (7): a fraction of the radiation emitted by the sample reflects off objects in the chamber such as the electrodes and heating mirror,

and off the chamber walls. A fraction of the reflected radiation finds it way back to the sample. Finally, a fraction of the radiation which finds its way back to the sample is reabsorbed, thereby reducing the radiative cooling rate. However, an approximate ray-tracing analysis accounting for the placement of the mirror and other reflective objects in the chamber shows that ignoring reflected and reabsorbed radiation will introduce an error of less than +2% in $c_p(T)/\varepsilon_T(T)$.

The area A(T) is computed from the temperature-dependent density, $\rho_l(T)$, available in the literature and shown in Table 1 [8]. The density data covers the temperatures range only above the melting point. However, they were extrapolated into the undercooked region in the present work. More accurate density data can easily be used to improve the accuracy of the present results in the future. In any case, the results are not very sensitive to the temperature variation of $\rho_l(T)$. For example, an error of ±100% in the expansion coefficient $\rho_\alpha(T_m)$ results in an error of only ±3%, ±10/0 and ±2% in $c_p(T)/\varepsilon_T(T)$ at the deepest undercooking levels of Ni, Zr, and Si, respectively.

Rearrangement o' Eq. (7) gives

$$\frac{c_p(T)}{\varepsilon_T(T)} = -\frac{\sigma A(T) M (T^4 - T_c^4)}{m \frac{dT}{dt}} \qquad (8)$$

The experimentally-obtained radiative cooling curves such as that shown in Figure 1 was smoothed and differentiated with respect to time using the Savitzky-Golay method [9] before inserting in the right hand side of Eq. (8). The Savitzky-Golay method was used because it maintains the derivative of the underlying data during smoothing. The amount of smoothing can be adjusted by changing the order of the smoothing polynomial or the width of the filtering window. A 3rd order polynomial and 0.2 s filter window were usually used for the present data.

Results

Fig. 3 shows the result of smoothing and differentiating the data falling between points #1 and #3 in Fig. 2. Only smoothed T(t) anti dT(t)/dt were used in applications of Eq. (8) to calculate $c_p(T)/\varepsilon_T(T)$ from the measured T(t). Several $c_p(T)/\varepsilon_T(T)$ curves were obtained for each material. For Ni, six curves were obtained from the same 19.4 mg sample. For Zr, three curves were obtained from the same 40.7 mg sample. For Si, one curve was obtained from a 31.9 mg sample, two were obtained from a 23.3 mg sample, one was obtained from a 8.9 mg sample, and one was obtained from a 17.2 mg sample, for a total of five. The final results shown in Figures 4, 5, and 6 were obtained by averaging all $c_p(T)/\varepsilon_T(T)$ curves for each material. Table 2 shows the formulas of least-squares curve fits through $c_p(T)/\varepsilon_T(T)$ and the temperature ranges over which they are valid, The uncertainty in $c_p(T)/\varepsilon_T(T)$ at a given T due to the effects described in the Measurement Approach section is estimated to be ±5%.

The constant pressure specific heat $c_p(T)$ can be found from Table 2 if $\varepsilon_T(T)$ is known simply by multiplying the formula evaluated at T by $\varepsilon_T(T)$. Similarly, the hemispherical total emissivity $\varepsilon_T(T)$ can be found if $c_p(T)$ is known. As an example of using the data in Figs. 4 through 6, the hemispherical total emissivity was determined for each liquid at its melting temperature. First, the ratios c_p/ε_T were evaluated at the material's melting temperature. These values were then used to find $\varepsilon_T(T_m)$ using the values of $c_p(T_m)$ available in the literature (Ni, Si: [8]; Zr: [1 O]) and they are shown in Table 3 .

There are very few published data to which the present values of ε_T can be compared. No ε_T data for Si could be found. Our previous work on liquid Zr [1 O] showed that the average ε_T between 2128 K (T_m) and 1769 K was 0.28+0.01, which agrees within experimental error with the present result, which is 0.29. Our previous

work on liquid Ni [1 O] showed that the average ε_T between 1728 K (T_m) and 1325 K was 0.1 6±0.01, which also coincides within experimental error to the present result, which is 0.15. Since c_p of Zr and Ni are not expected to vary greatly with temperature, and since $c_p(T)/\varepsilon_T(T)$ shown in Figs. 4 and 5 does not vary greatly with T, it is not surprising that ε_T averaged throughout the undercooked region is almost the same as $\varepsilon_T(T_m)$.

During electrostatic levitation, a finite normal electric field exists at the surface of the sample of the order of 10^6 V/m. It is possible that the electric field affects ε_T even though it only penetrates into a thin layer near the surface. Electrons which are responsible for emission of electromagnetic radiation are also located near the surface. Those electrons must respond to the electrostatic field as they undergo motions which result in the emission of radiation. 'l"he possible influence of electrostatic fields on ε_T will be investigated in the future.

Note that the ratio c_p/ε_T shows a marked decrease with increasing temperature for liquid silicon (Fig. 6), while the same ratio is almost constant for nickel and zirconium (Figs. 4 and 5). In a related work which is to be published separately we show how the temperature-dependence of the ratio c_p/ε_T is due to changes in short-range atomic order in these undercooked metallic melts.

Acknowledgements

The authors would like to thank Mr. Craig Morton of Vanderbilt University, Nashville, TN, for preparing the zirconium sample and recommending the cleaning treatment. We are also indebted to Professor William Hofmeister of Vanderbilt University for helpful discussions on optical pyrometry. This work was carried out at the Jet Propulsion Laboratory, California Institute of Technology, under contract with the National Aeronautics and Space Administration.

	T_m (K)	$\rho_l(T_m)$ (kg/m^3)	$\rho_\alpha(T_m)$ (kg/m^3/K)
Ni	1728	7900	-1.19
Zr	2128	5930	-0.32
Si	1687	2530	-0.35

Table 1. Properties of liquid Ni, Zr, and Si. The liquid density is $\rho_l(T) = \rho_l(T_m) + \rho_\alpha(T_m)(T - T_m)$ [8].

	c_p/ε_T ((J mol^{-1} K^{-1}))	range (K)
Ni	423,0 - 0.09622•T	1460 to 1740
Zr	176,0 - 0.01669•T	1825 to 2140
Si	134.5 + 1.261×10^7 *exp*(-0.008171•T)	1450 to 1880

Table 2. Curve fits for c_p/ε_T (J mol^{-1} K-l) vs. T (K) for liquid materials. The uncertainty in $c_p(T)/\varepsilon_T(T)$ at a given T is estimated to be ±5%. Note the temperature range over which the curves are valid. These curves are plotted in Figs. 4 through 6.

	$c_p(T_m)$ (J/mol/K)	$\varepsilon_T(T_m)$
Ni	38.5	0.15±0.01
Zr	40.8	0.29±0.01
Si	25.61	0.17±0.01

Table 3. Properties of liquid Ni, Zr, and Si at their melting temperatures. Calculation of $\varepsilon_T(T_m)$ using published $c_p(T_m)$ values (Ni, Si: [8]; Zr: [10]).

References

1. F. Spaepen: *Science,* 1987, 235, 1010.

2. R. Siegel and J. R. Howell: *Thermal Radiation Heat Transfer,* 2nd cd., Hemisphere Publishing Company, New York, 1981.

3. A. J. Sievers: *J. Opt.* Sot. Am., 1978, 68(11), 1505.

4. W. K. Rhim, S. K. Chung, D. Barber, K. F. Man, G. Gutt, A. Rulison, and R. E. Spjut: *Rev. Sci. Instr.*, 1993, 64(1 O), 2961.

5. W. H. Hofmeister, R. J. Bayuzick, and M. B. Robinson, Rev. Sci. Instrum., 1990, 61 (8), 2220.

6. S. Krishnan, J. K. R. Weber, P. C. Nordine, R. A. Schiffman, R. H. Hauge and J. L. Margrave: *High Temperature* Science, 1991, 30, 137.

7. R. Smalley and A. J. Sievers: *J. Opt.* Sot. *Am., 1978, 68(1* 1), 1516.

8. T. Iida, and R. 1. L. Guthrie: *The Physical Properties of Liquid Metals,* Clarendon Press, Oxford, 1988.

9. W. H. Press, S. A. Teukolsky, W. T. Vetterling, and B. P. Flannery: *Numerical Recipes in C,* Cambridge University Press, Cambridge, 1992.

10. A. J. Rulison and W. K. Rhim: *Rev. Sci. Instr.*, 1994, 65(3), 695.

Figure Captions

1. Sketch of the sample with surrounding electrodes drawn approximately to scale.

2. Temperature vs. time during radiative cooling of a 19.4 mg nickel sample. Unsoothed data.

3. Smoothed temperature versus time and first derivative of temperature vs. time resulting from applying the Savitzky-Golay filter to the data appearing between points #1 and #3 in Fig. 1.

4. Ratio of constant-pressure specific heat to hemispherical total emissivity vs. temperature for liquid nickel in vacuum. Long dashes: experiment. Solid: least squares curve fit. Short dashes: ±5% of curve fit.

5. Ratio of constant-pressure specific heat to hemispherical total emissivity vs. temperature for liquid zirconium in vacuum. Long dashes: experiment. Solid: least squares curve fit. Short dashes: ±5% of curve fit.

6. Ratio of constant-pressure specific heat to hemispherical total emissivity vs. temperature for liquid silicon in vacuum. Long dashes: experiment. Solid: least squares curve fit. Short dashes: ±5% of curve fit.

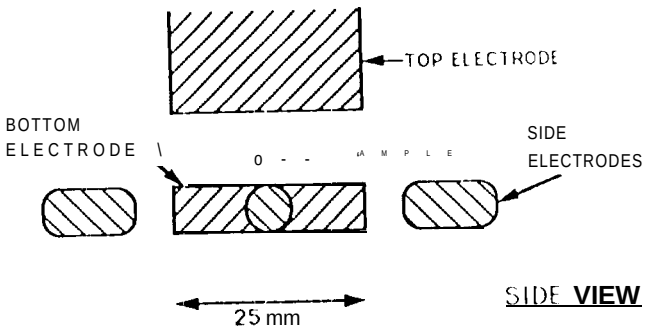

SIDE VIEW

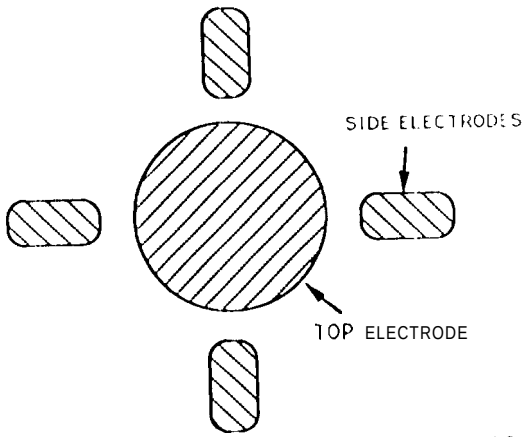

TOP VIEW

Fig 1

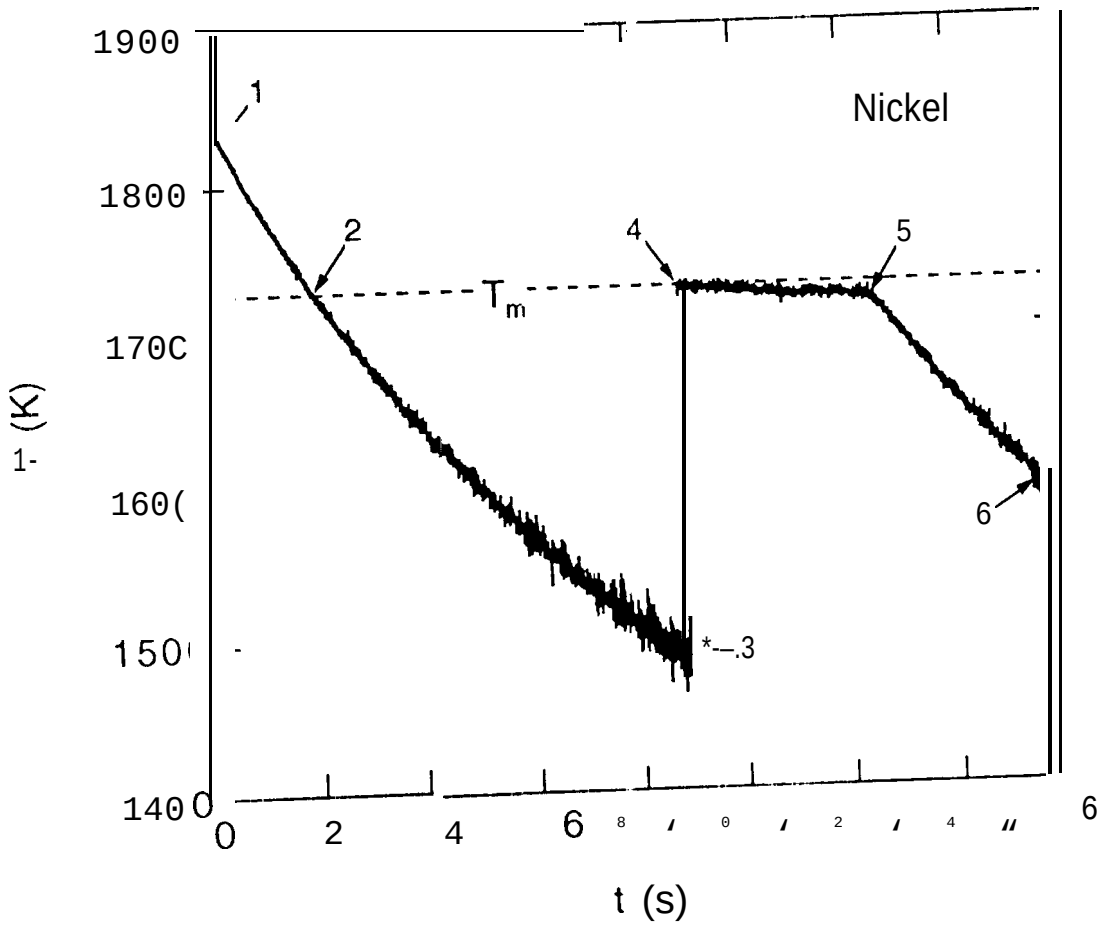

Rulison and Rhim Fig. 2

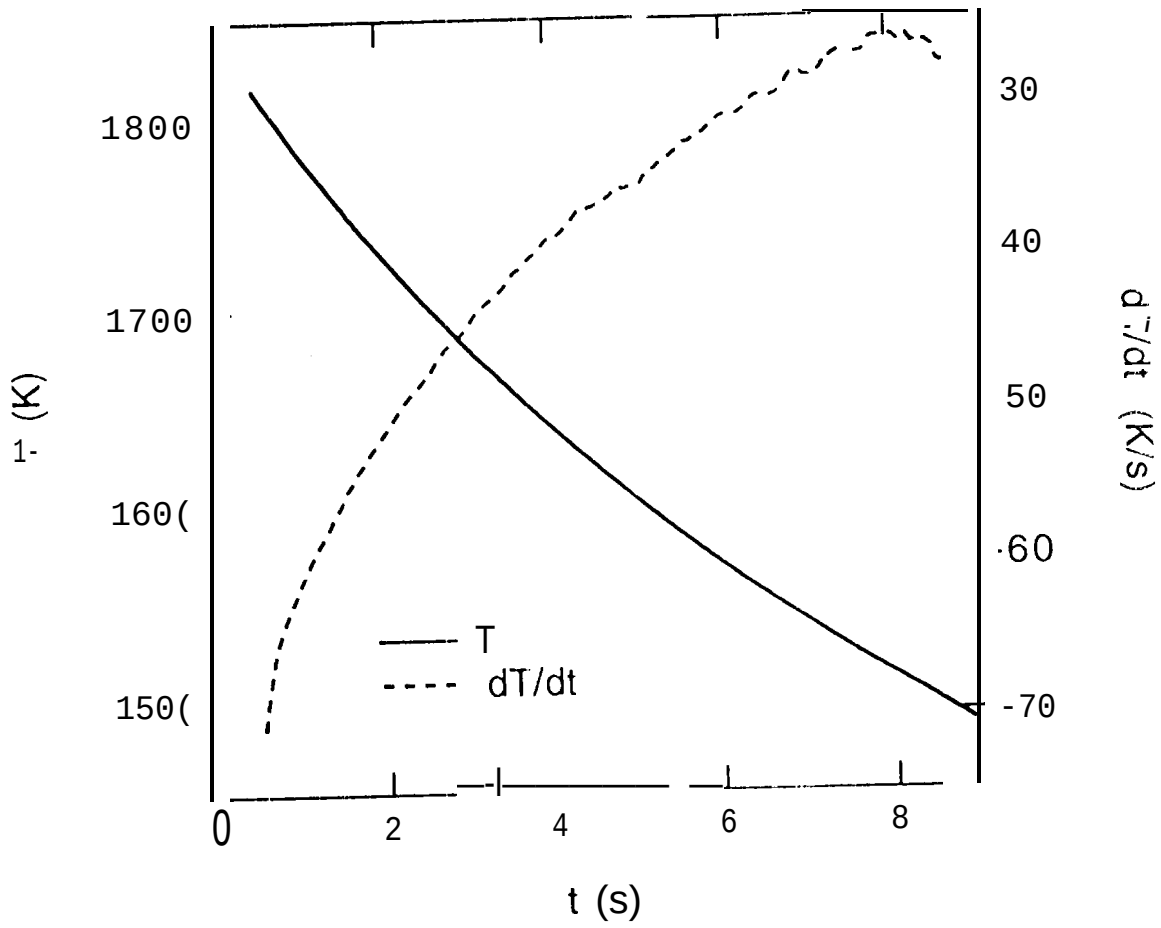

Rulison and Rhim Fig. 3

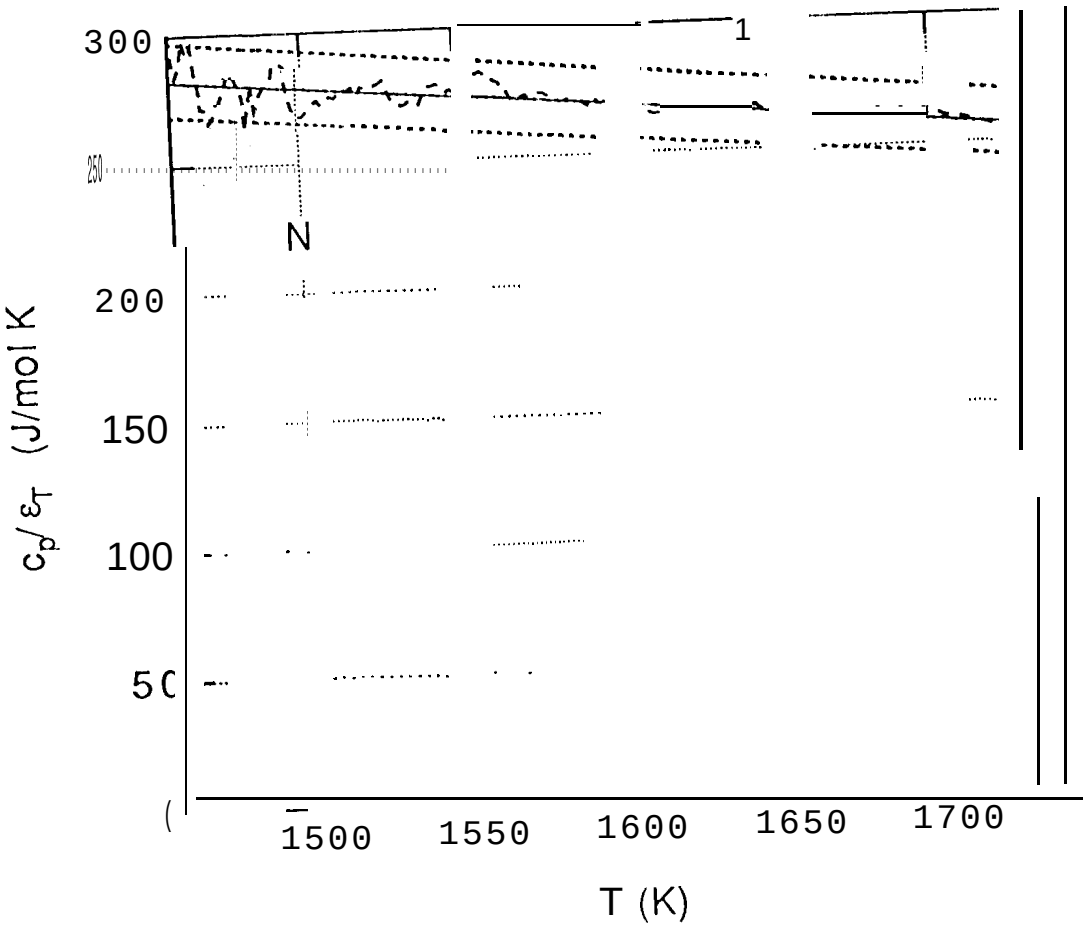

Rulison and Rhim, Fig. B4

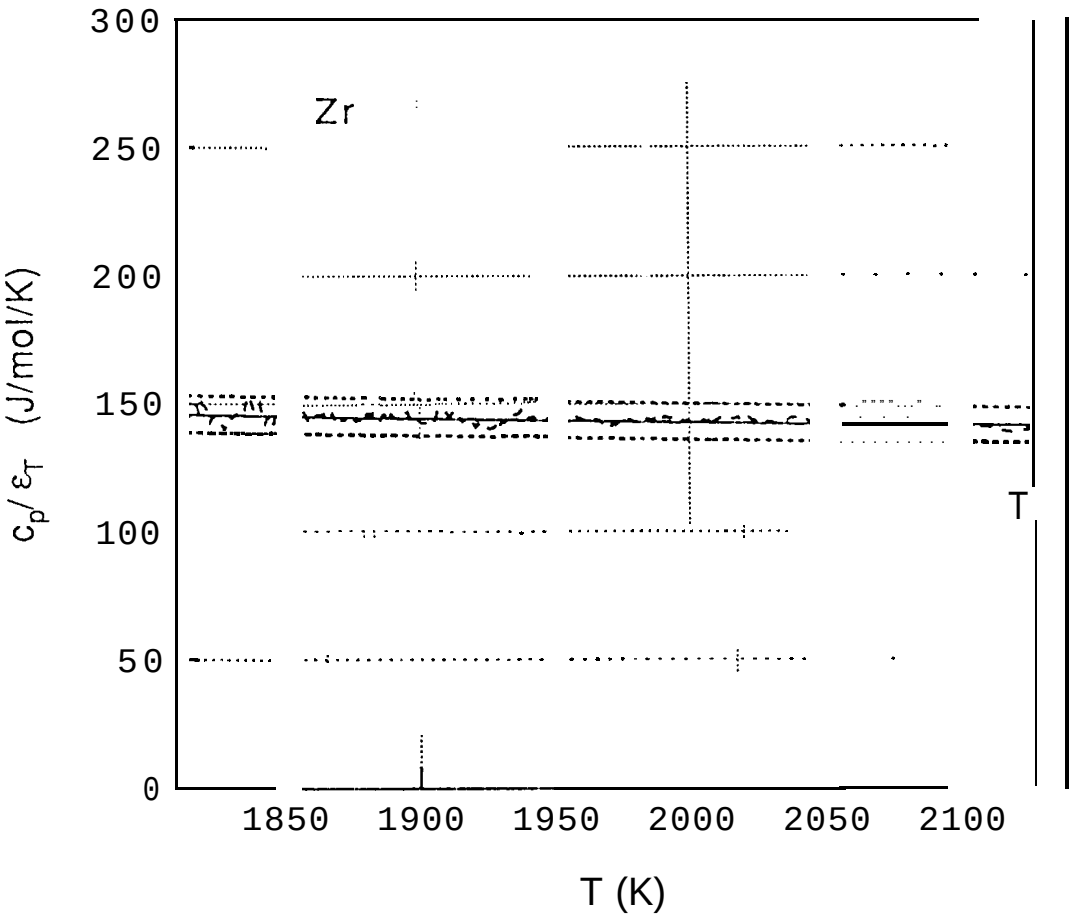

Rulison and Rhim, Fig. #5

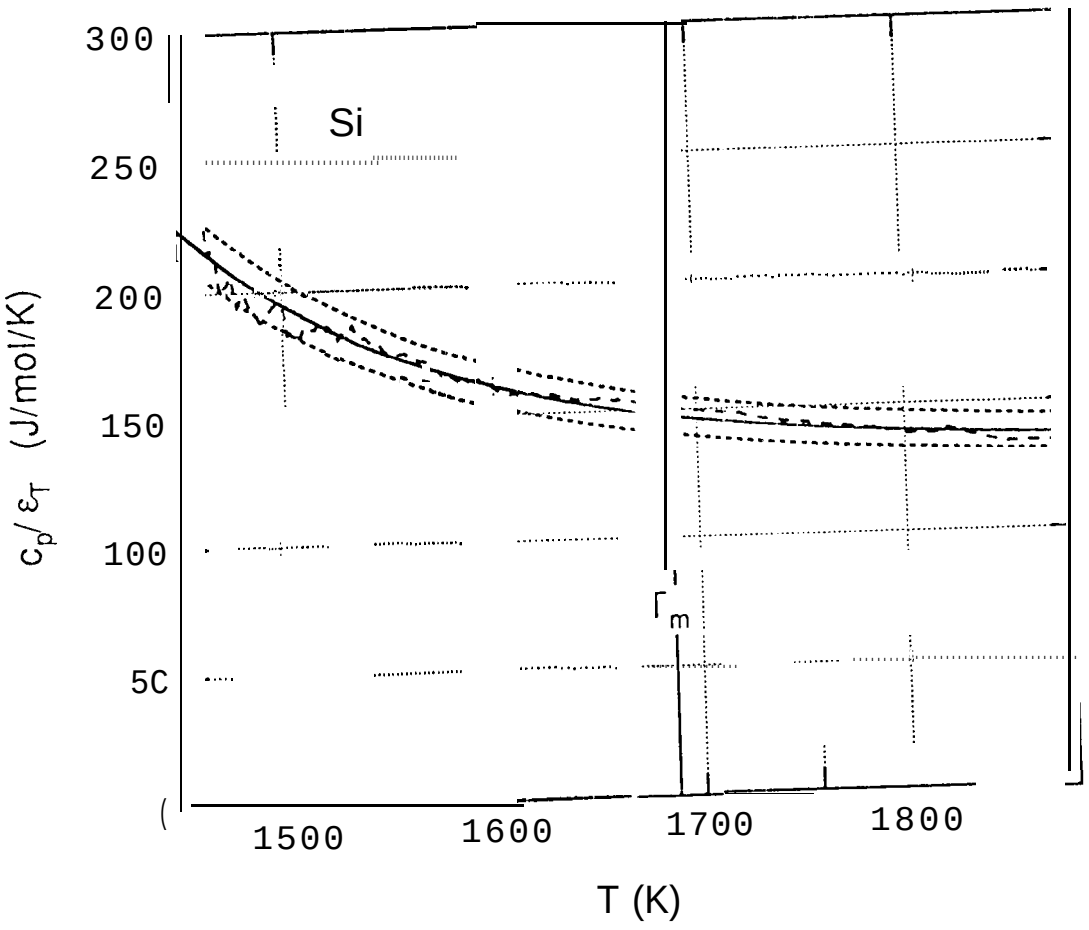

Rulison and Rhim, Fig. #6